

Scaling behaviors of branched polymers

Hajime Aoki,^{1,*} Satoshi Iso,^{2,†} Hikaru Kawai,^{3,‡} and Yoshihisa Kitazawa^{2,§}

¹*Department of Physics, Saga University, Saga 840-8502, Japan*

²*High Energy Accelerator Research Organization (KEK), Tsukuba, Ibaraki 305, Japan*

³*Department of Physics, Kyoto University, Kyoto 606-8502, Japan*

(Received 8 May 2000)

We study the thermodynamic behavior of branched polymers. We first study random walks in order to clarify the thermodynamic relation between the canonical ensemble and the grand canonical ensemble. We then show that correlation functions for branched polymers are given by those for ϕ^3 theory with a single mass insertion, not those for the ϕ^3 theory themselves. In particular, the two-point function behaves as $1/p^4$, not as $1/p^2$, in the scaling region. This behavior is consistent with the fact that the Hausdorff dimension of the branched polymer is 4. In the appendixes we derive the exact two-point correlation function at finite (but large) system size N , which is consistent with the analysis in the body of the paper.

PACS number(s): 05.40.Fb, 61.82.Pv

I. INTRODUCTION

Branched polymers are the simplest generalization of the random walk, and have been studied extensively (see, for example, Ref. [1]). They are of great importance not only in statistical physics but also in particle physics, in particular, for understanding the critical behavior of random surfaces and quantum gravity [2–4]. Our recent interest in branched polymers arose from our attempt to formulate superstring theory nonperturbatively. In Ref. [5], we studied the dynamics of a type IIB matrix model in such a framework (see Ref. [6] and also see Ref. [7] for review). In our matrix model approach, the eigenvalues of matrices were interpreted as space-time coordinates. In these investigations, we found the system of branched polymers in a simple approximation. Although it is far from the flat four-dimensional manifold, branched polymers share the same (fractal) dimensionality 4 with our space-time coordinates. This might be the first indication that superstring theory can explain the dimensionality of our space-time.

In this paper, we comment on a field theoretic description of branched polymers. It is well known that a system of random walks is described by free scalar field theory if there is no effect of self-avoidance. Similarly, it is widely believed that a system of branched polymers is described by a scalar field theory with a three-point coupling, that is, ϕ^3 scalar field theory. However, we will show that this is not so by treating the universal part of the partition function carefully. A system of branched polymers without self-avoidance can be exactly solvable by introducing the grand canonical ensemble and using the so called Schwinger-Dyson technique. In order to extract the correct large N limit (N is the system size) or the thermodynamic limit, we have to check that the grand canonical ensemble is dominated by the larger size system. In other words, we have to extract the universal part.

Our claim is that we need a single mass insertion in each m -point correlation function of the ϕ^3 scalar field theory in order to describe m -point correlation functions in branched polymers. Mass insertion here means a change of a propagator in each m -point function from an ordinary one, $1/p^2$, to $1/p^4$. In particular, the two-point function behaves as $1/p^4$, not $1/p^2$. Let us count the number of points which lie within distance R from a fixed point in d (>4) dimensions. In the random walk, this can be estimated as R^2 by using the two-point function. We obtain R^4 for branched polymers by using a $1/p^4$ type propagator. This our findings are consistent with the claim that branched polymers are four-dimensional fractals. A multipoint correlation function is given by a sum of graphs of the corresponding correlation function for ϕ^3 scalar field theory at tree level, with a single mass insertion in each graph.

Our main results were announced in Ref. [9]. In this paper we would like to give a fuller account of our results by providing more detailed derivations and explanations. The organization of this paper is as follows. In Sec. II, we review random walks in order to clarify the relation between the canonical and grand canonical ensemble. In Sec. III, we investigate branched polymers. First we define a canonical ensemble for a system of branched polymers (Sec. III A), and then introduce grand canonical ensembles (Sec. III B). We emphasize that the definition of a grand canonical ensemble is not unique. In Sec. III C, we solve Schwinger-Dyson equations for the conventional grand canonical ensemble, and obtain results which correspond to the correlation functions of a scalar ϕ^3 theory. In Sec. III D, we consider the thermodynamic limit of the correlation functions, and obtain the correct universal behavior of these. In Sec. IV, we give a physical interpretation of why the propagator behaves $1/p^4$ in branched polymers. Section V is devoted to conclusions and discussions. We have two appendixes A and B which derive the partition function and the two-point function in the canonical ensemble of branched polymers. In Appendix B we derive the two-point correlation function exactly at a finite system size N . The result is consistent with the analysis in Sec. III in the scaling region.

*Email address: haoki@cc.saga-u.ac.jp

†Email address: satoshi.iso@kek.jp

‡Email address: hkawai@gauge.scphys.kyoto-u.ac.jp

§Email address: kitazawa@post.kek.jp

II. RANDOM WALKS

In this section, we give a brief introduction to random walks in order to clarify the thermodynamic relation between the canonical and grand canonical ensemble. The canonical partition function with the system size N is given by

$$Z_N = \int \prod_{i=1}^N d^d y^i \prod_{i=1}^{N-1} f(y^i - y^{i+1}) = V(\hat{f}(0))^{N-1}, \quad (2.1)$$

where V is the total volume of the system, and $f(x)$ is a function assigned to each bond that damps sufficiently quickly at long distances compared to the typical length scale a_0 . $\hat{f}(p)$ is its Fourier transform:

$$\hat{f}(p) = \int d^d x e^{ipx} f(x). \quad (2.2)$$

For example, we can take $f(x) = \exp[-(x/a_0)^2/2]$.

Correlation functions for density $\rho(x) = \sum_{i=1}^N \delta^{(d)}(x - y^i)$ can be easily calculated. The one-point function becomes

$$\begin{aligned} \langle \rho(x) \rangle_N &= \frac{1}{Z_N} \int \prod_{i=1}^N d^d y^i \prod_{i=1}^{N-1} f(y^i - y^{i+1}) \sum_{i=1}^N \delta^{(d)}(x - y^i) \\ &= \frac{N}{V}. \end{aligned} \quad (2.3)$$

The two-point function is defined as

$$\begin{aligned} \langle \rho(x^1) \rho(x^2) \rangle_N &= \frac{1}{Z_N} \int \prod_{i=1}^N d^d y^i \prod_{i=1}^{N-1} f(y^i - y^{i+1}) \\ &\quad \times \sum_{i=1}^N \delta^{(d)}(x^1 - y^i) \sum_{j=1}^N \delta^{(d)}(x^2 - y^j), \end{aligned} \quad (2.4)$$

and its Fourier transformation is given by

$$\begin{aligned} \hat{g}_N^{(2)}(p) &= \int d^d x \langle \rho(x) \rho(0) \rangle_N e^{-ipx} \\ &= \frac{1}{Z_N} \left(\sum_{i,j} (\hat{f}(p))^{i-j} (\hat{f}(0))^{N-|i-j|-1} \right) \\ &= \frac{1}{V} \sum_{i,j} \left(\frac{\hat{f}(p)}{\hat{f}(0)} \right)^{|i-j|} \\ &= \frac{2}{V} \sum_{s=0}^{N-1} (h(p))^s (N-s) - \frac{N}{V} \\ &= \frac{2N}{V(1-h(p))} \left(1 - \frac{h(p)[1-h(p)^N]}{N[1-h(p)]} \right) - \frac{N}{V} \\ &= \frac{2N}{VH(p)} \left(1 - \frac{1-e^{-NH(p)}}{NH(p)} \right) \left(1 + O\left(\frac{1}{N}, H(p)\right) \right), \end{aligned} \quad (2.5)$$

where

$$h(p) \equiv \hat{f}(p)/\hat{f}(0) = \exp[-(a_0 p)^2/2], \quad (2.6)$$

$$H(p) \equiv 1 - h(p) = (a_0 p)^2/2 + \dots \quad (2.7)$$

We can approximate the two-point function as

$$\hat{g}_N^{(2)}(p) = \frac{2N}{V} \frac{1}{H(p)} \left(1 - \frac{1}{NH(p)} + O\left(\frac{1}{[NH(p)]^2}\right) \right) \quad (2.8)$$

in the scaling region

$$\frac{1}{N} < H(p) \ll 1 \quad (2.9)$$

or

$$N^{-1/2}/a_0 < p \ll 1/a_0. \quad (2.10)$$

The scaling region is between the ultraviolet cutoff scale a_0 and the infrared scale of the system extent, which is given by $\xi = a_0 N^{1/2}$.

The two-point correlation function is also calculated in the grand canonical ensemble. A conventional grand canonical partition function is given as

$$Z_{\kappa_0} = \sum_{N=1}^{\infty} \kappa_0^N Z_N = \frac{V \kappa_c \kappa_0}{\kappa_c - \kappa_0}, \quad (2.11)$$

where κ_0 is the fugacity, and $\kappa_c = (\hat{f}(0))^{-1}$. For later convenience, we first define an unnormalized two-point function by

$$\begin{aligned} \hat{G}_{\kappa_0}^{(2)}(p) &= \sum_{N=1}^{\infty} \kappa_0^N \sum_{i,j} (\hat{f}(p))^{i-j} (\hat{f}(0))^{N-|i-j|-1} \\ &= \frac{\kappa_0}{(1-\kappa_0)^2} \frac{2}{[1-\kappa_0 \hat{f}(p)]} - \frac{\kappa_0}{[1-\kappa_0 \hat{f}(0)]^2} \\ &= \frac{\kappa_0 \kappa_c^3}{(\kappa_c - \kappa_0)^2} \frac{2}{[\kappa_c - \kappa_0 h(p)]} - \frac{\kappa_0 \kappa_c^2}{(\kappa_c - \kappa_0)^2}. \end{aligned} \quad (2.12)$$

Hence the normalized two-point function becomes

$$\begin{aligned} \hat{g}_{\kappa_0}^{(2)}(p) &\equiv \frac{\hat{G}_{\kappa_0}^{(2)}(p)}{Z_{\kappa_0}} \\ &= \frac{1}{V[1-\kappa_0 \hat{f}(0)]} \frac{2}{[1-\kappa_0 \hat{f}(p)]} - \frac{1}{V} \frac{\kappa_c}{\kappa_c - \kappa_0} \\ &= \frac{2\kappa_c}{V\delta\kappa} \frac{1}{[1-h(p)] + \frac{\delta\kappa}{\kappa_c} h(p)} - \frac{1}{V} \frac{\kappa_c}{\delta\kappa} \\ &= \frac{2\kappa_c}{V\delta\kappa} \frac{1}{H(p) + \frac{\delta\kappa}{\kappa_c}} \left(1 + O\left(\frac{\delta\kappa}{\kappa_c}, H(p)\right) \right), \end{aligned} \quad (2.13)$$

where $\delta\kappa = \kappa_c - \kappa_0$. Since $\langle N \rangle = \kappa_c / \delta\kappa$, the correlation function behaves as that of massive scalar particles

$$\hat{g}^{(2)}(p)_{\kappa_0} \sim \frac{2\langle N \rangle}{V} \frac{1}{H(p) + 1/\langle N \rangle}, \quad (2.14)$$

and agrees with the result in the canonical ensemble calculation. This result gives the correlation length $\xi = a_0 N^{1/2}$, which indicates the Hausdorff dimension of random walk $d_H = 2$.

Here we give two different definitions of Hausdorff dimensions. The first one is defined in terms of the relation between the system size N and the extent of the system. The infrared behavior of the above two-point function shows that the correlation damps rapidly over the length scale $\xi = a_0 N^{1/2}$. Since the extent of the system $L \sim \xi$ is proportional to $N^{1/2}$, the Hausdorff dimension is given by $d_H^{(1)} = 2$, where $d_H^{(1)}$ is defined as

$$L = a_0 N^{1/d_H^{(1)}}. \quad (2.15)$$

The second definition is to use the behavior of the correlation function at much shorter length scale than the system size $L = \xi$. In d -dimensional coordinate space, the density correlation behaves as

$$g^{(2)}(x) \sim \frac{\exp(-m|x|)}{|x|^{d-2}}, \quad (2.16)$$

where $m = 1/\xi$. If $|x| \ll 1/m$, the mass term can be neglected and $g^{(2)}(x) \sim 1/|x|^{d-2}$. The total number of points within a ball of radius R ($R \ll L$) around a certain point is evaluated as

$$N(R) = \int^R d^d x g^{(2)}(x) \sim \left(\frac{R}{a_0}\right)^2, \quad (2.17)$$

and gives the Hausdorff dimension $d_H^{(2)} = 2$. Here the definition of $d_H^{(2)}$ is

$$N(R) = \left(\frac{R}{a_0}\right)^{d_H^{(2)}}. \quad (2.18)$$

The second definition of the Hausdorff dimension is determined only through the behavior of correlation functions in the scaling region $a_0 \ll x \ll \xi$, and has nothing to do with the behaviors near the infrared cutoff. Hence it is a more appropriate definition than the first one from the thermodynamic viewpoint. Of course, it is quite natural that we should obtain the same dimension d_H from the both definitions, since the extent of the system is approximately evaluated at the length L where $N(L) = N$.

Finally in this section, we comment on generalized types of grand canonical ensembles. Since the motivation of introducing grand canonical ensembles is to reproduce the same thermodynamic quantities as those in the canonical one, we may assign different weights in summing over different N . We define generalized grand canonical ensembles by

$$Z_{\kappa_0, l} = \sum_{N=1}^{\infty} N^l \kappa_0^N Z_N, \quad (2.19)$$

$$\hat{G}_{\kappa_0, l}^{(2)}(p) = \sum_{N=1}^{\infty} N^l \kappa_0^N \hat{G}_N^{(2)}(p),$$

where κ_0 is the fugacity. Here we assign an extra N -dependent factor N^l , in addition to the usual one, κ_0^N . The criterion for a ‘‘good’’ grand canonical ensemble is such that we can take the correct thermodynamic limit, or, in other words, correctly take the universal part in the sum over N . That is, the correlation functions in the grand canonical ensemble at the critical value of fugacity should reproduce those in the canonical ensemble for large N :

$$\lim_{N \rightarrow \infty} g_N^{(2)} = \lim_{\kappa_0 \rightarrow \kappa_{0,c}} g_{\kappa_0, l}^{(2)}. \quad (2.20)$$

This criterion holds if the grand canonical ensemble is dominated by large N systems. If the above criterion is satisfied for some value of l , it does hold for larger values of l . As we will see in Sec. III, we need to introduce the generalized ensembles of $l > 0$ to satisfy the criterion in branched polymer systems. However, in the case of random walks, this already holds for the conventional grand canonical ensemble of $l = 0$, and we do not need to introduce the generalized ones.

From Eqs. (2.11) and (2.12), the generalized partition functions and the correlation functions are given by

$$Z_{\kappa_0, l} = \left(\kappa_0 \frac{\partial}{\partial \kappa_0}\right)^l Z_{\kappa_0}, \quad (2.21)$$

$$\hat{G}_{\kappa_0, l}^{(2)}(p) = \left(\kappa_0 \frac{\partial}{\partial \kappa_0}\right)^l \hat{G}_{\kappa_0}^{(2)}.$$

We are interested in behaviors near the critical point $\delta\kappa \sim 0$ ($N \rightarrow \infty$) and in the scaling region where $1/(\kappa_c - \kappa_0) > 1/(\kappa_c - h(p)\kappa_0) \gg 1/\kappa_c$. In this region, they become

$$\begin{aligned} Z_{\kappa_0, l} &\sim \frac{V \kappa_c^{l+2} l!}{(\kappa_c - \kappa_0)^{l+1}}, \\ \hat{G}_{\kappa_0, l}^{(2)}(p) &\sim \frac{2 \kappa_c^{l+4} (l+1)!}{[\kappa_c - h(p)\kappa_0] (\kappa_c - \kappa_0)^{l+2}} \\ &\quad \times \left(1 + \frac{l}{l+1} \frac{\kappa_c - \kappa_0}{\kappa_c - h(p)\kappa_0} + \dots\right) \\ &\sim \frac{2 \kappa_c^{l+4} (l+1)!}{(\kappa_c - \kappa_0)^{l+2}} \frac{1}{\kappa_0 H(p)} \\ &\quad \times \left(1 - \frac{\delta\kappa}{(l+1)\kappa_0} \frac{1}{H(p)} + \dots\right). \end{aligned} \quad (2.22)$$

Since $\langle N \rangle = Z_{\kappa_0, l+1} / Z_{\kappa_0, l} = \kappa_c (l+1) / \delta\kappa$ for the generalized grand canonical ensembles of l , the normalized correlation functions become

$$\hat{g}_{\kappa_0, l}^{(2)}(p) \sim \frac{2\langle N \rangle}{V} \frac{1}{H(p)} \left(1 - \frac{1}{\langle N \rangle H(p)} + \dots \right), \quad (2.23)$$

which agrees with the previous result [Eq. (2.14)] of $l=0$.

III. BRANCHED POLYMER DYNAMICS

A. Canonical ensemble

Branched polymers are a statistical system of N points connected by $N-1$ bonds whose lengths are of order a_0 . The canonical partition function is defined as

$$Z_N = \frac{1}{N!} \sum_{G: \text{tree graph}} \int \prod_{i=1}^N d^d y^i \prod_{(ij): \text{bond of } G} f(y^i - y^j), \quad (3.1)$$

where $f(x)$ is a function assigned to each bond in each graph, and it damps sufficiently fast at long distances compared to the typical length scale a_0 . The presence of the factor $1/N!$ is due to the fact that the N points are regarded identical.

We can calculate a partition function for each N , by counting the number of all possible tree graphs:

$$\begin{aligned} Z_1 &= V, \\ Z_2 &= \frac{1}{2!} \hat{f}(0) V, \\ Z_3 &= \frac{1}{3!} 3 \hat{f}(0)^2 V, \\ Z_4 &= \frac{1}{4!} 16 \hat{f}(0)^3 V, \\ &\vdots \\ Z_N &= \frac{1}{N!} N^{N-2} \hat{f}(0)^{N-1} V, \end{aligned} \quad (3.2)$$

where $\hat{f}(p)$ is a Fourier transform of $f(x)$,

$$\hat{f}(p) = \int d^d x e^{ipx} f(x), \quad (3.3)$$

and V is the total volume of the system. A derivation of the general form of Eq. (3.2) is given in Appendix A.

We define an (unnormalized) m -point correlation function of density operators as

$$\begin{aligned} G_N^{(m)}(x^1, \dots, x^m) &= Z_N \langle \rho(x^1) \cdots \rho(x^m) \rangle_N \\ &= \frac{1}{N!} \sum_{G: \text{tree graph}} \int \prod_{i=1}^N d^d y^i \prod_{(ij): \text{bond of } G} \\ &\quad \times f(y^i - y^j) \rho(x^1) \cdots \rho(x^m), \end{aligned} \quad (3.4)$$

where the density operator is defined by

$$\rho(x) = \sum_{i=1}^N \delta^{(d)}(x - y^i). \quad (3.5)$$

Due to the translational invariance, the one-point function is proportional to the partition function:

$$G_N^{(1)} = \frac{N}{V} Z_N. \quad (3.6)$$

The one-point function is nothing but the partition function with one marked point.

B. Grand canonical ensemble

We then define partition functions and m -point correlation functions in the generalized grand canonical ensembles as in Sec. II:

$$Z_{\kappa_0, l} = \sum_{N=1}^{\infty} N^l \kappa_0^N Z_N, \quad (3.7)$$

$$G_{\kappa_0, l}^{(m)}(x^1, \dots, x^m) = \sum_{N=1}^{\infty} N^l \kappa_0^N G_N^{(m)}(x^1, \dots, x^m). \quad (3.8)$$

κ_0 is the fugacity.

The criterion for a ‘‘good’’ grand canonical ensemble is such that we can take the correct thermodynamic limit in the following sense. The correlation functions in the grand canonical ensemble at the critical value of fugacity should reproduce those in the canonical ensemble for large N ,

$$\lim_{N \rightarrow \infty} g_N^{(m)} = \lim_{\kappa_0 \rightarrow \kappa_{0,c}} g_{\kappa_0, l}^{(m)}, \quad (3.9)$$

where we have defined normalized correlation functions as

$$g_N^{(m)} = \frac{G_N^{(m)}}{Z_N}, \quad g_{\kappa_0, l}^{(m)} = \frac{G_{\kappa_0, l}^{(m)}}{Z_{\kappa_0, l}}. \quad (3.10)$$

In the case of random walks, we have confirmed that this does hold for any non-negative value of l , but we need to check it in the case of branched polymers. To satisfy this criterion, the grand canonical ensembles with N -dependent weights should be dominated by large N systems. This is not assured only by taking the fugacity near the critical value. This is because, if $G_N^{(m)}$ behaves like $(\kappa_{0,c})^{-N} N^\alpha$ for large N and $l + \alpha < -1$, the summation over N is dominated by a small N system, not by the large $N \sim \kappa_c / \Delta \kappa$ even near the critical point. On the other hand, if we take a sufficiently large l , we can obtain the correct large N correlation functions in the grand canonical ensembles, which are, of course, independent of l .

We illustrate the above mentioned criterion by taking the partition function as an example. Since the canonical ensemble partition function (3.2) behaves at large N as

$$Z_N \sim \frac{N^{-5/2}}{\sqrt{2\pi e}^{-N}} \hat{f}(0)^{N-1} V, \quad (3.11)$$

the grand canonical ensemble is approximated by

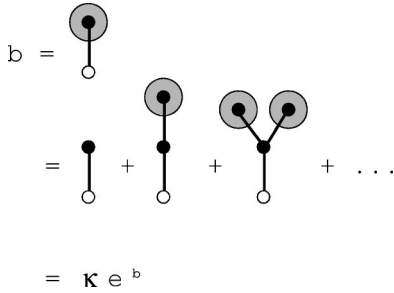


FIG. 1. Schwinger-Dyson equation for the one point function. The gray blob and black point mean $\hat{G}_{\kappa_0}^{(1)}$ and κ_0 , respectively.

$$Z_{\kappa_0, l} \sim \frac{V}{\sqrt{2\pi\hat{f}(0)}} \sum_{N=1}^{\infty} N^{l-5/2} (\kappa/\kappa_c)^N$$

$$\sim \frac{V}{\sqrt{2\pi\hat{f}(0)}} \int_0^{\infty} dN N^{l-5/2} e^{-N\Delta\kappa/\kappa_c}, \quad (3.12)$$

where

$$\kappa = \hat{f}(0)\kappa_0,$$

$$\kappa_c = e^{-1}, \quad (3.13)$$

$$\Delta\kappa = \kappa_c - \kappa.$$

If we take l sufficiently large, the integrand in Eq. (3.12) has a peak at $N \sim \kappa_c/\Delta\kappa$, and we can make $\langle N \rangle$ large by letting κ approach κ_c . On the other hand, if l is not sufficiently large, a nonuniversal small N behavior dominates the summation, and we cannot obtain the correct answer of the large N limit by a grand canonical ensemble.

C. Schwinger-Dyson equation

In this subsection, we recapitulate the arguments that the correlation functions for branched polymers in the conventional grand canonical ensemble are given by massless ϕ^3 theory. Let us consider the correlation functions $G_{\kappa_0}^{(m)} = G_{\kappa_0, l=0}^{(m)}$, which are suitable for Schwinger-Dyson analysis:

$$G_{\kappa_0}^{(m)}(x^1, \dots, x^m) = \sum_{N=1}^{\infty} \kappa_0^N G_N^{(m)}(x^1, \dots, x^m). \quad (3.14)$$

We write a Fourier transform of $G_{\kappa_0}^{(m)}(x^1, \dots, x^m)$ as $\hat{G}_{\kappa_0}^{(m)}(p^1, \dots, p^{m-1})$:

$$(2\pi)^d \delta^{(d)}(p^1 + \dots + p^m) \hat{G}_{\kappa_0}^{(m)}(p^1, \dots, p^{m-1})$$

$$= \int d^d x^1 \dots d^d x^m e^{ip^1 x^1} \dots e^{ip^m x^m} G_{\kappa_0}^{(m)}(x^1, \dots, x^m). \quad (3.15)$$

The Schwinger-Dyson equation for the one-point function $\hat{G}_{\kappa_0}^{(1)}$ becomes

$$b = \kappa e^b, \quad (3.16)$$

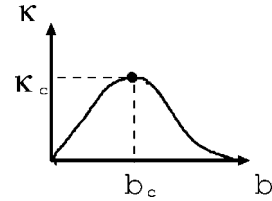


FIG. 2. Schwinger-Dyson equation $\kappa = b e^{-b}$. At the critical point, $b_c = 1$ and $\kappa_c = e^{-1}$.

where

$$b \equiv \hat{f}(0)\hat{G}_{\kappa_0}^{(1)}, \quad (3.17)$$

as can be seen from Fig. 1.

At the critical point, as illustrated in Fig. 2,

$$b_c = 1,$$

$$\kappa_c = e^{-1}, \quad (3.18)$$

$db/d\kappa$ diverges. Near this critical point, $\langle N \rangle$ becomes large,

$$\Delta b \sim \sqrt{2e} \sqrt{\Delta\kappa} \sim 1/\sqrt{\langle N \rangle}, \quad (3.19)$$

where

$$\Delta b = b_c - b,$$

$$\Delta\kappa = \kappa_c - \kappa. \quad (3.20)$$

The one-point function (which is equal to the partition function of $l=1$) now behaves as follows:

$$Z_{\kappa_0, l=1} = \sum_N N \kappa_0^N Z_N = V \sum_N \kappa_0^N G_N^{(1)} = V \hat{G}_{\kappa_0}^{(1)}$$

$$= \frac{bV}{\hat{f}(0)} \sim \frac{V}{\hat{f}(0)} (1 - \sqrt{2e} \sqrt{\Delta\kappa}). \quad (3.21)$$

Next we consider the two-point function $\hat{G}_{\kappa_0}^{(2)}(p)$. When we pick up any two points on a tree graph, we can fix the path connecting these two points. Thus, as can be seen from Fig. 3, the two-point function is calculated to be

$$\hat{G}_{\kappa_0}^{(2)}(p) = \sum_{s=0}^{\infty} \hat{f}(p)^s (\hat{G}_{\kappa_0}^{(1)})^{s+1}$$

$$= \frac{b}{\hat{f}(0)[1 - bh(p)]}, \quad (3.22)$$

where

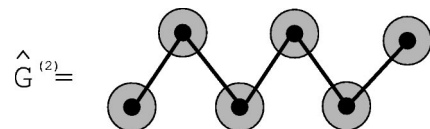


FIG. 3. The two-point function $\hat{G}_{\kappa_0}^{(2)}$ is created from the one-point function $\hat{G}_{\kappa_0}^{(1)}$, which is shown by a gray blob.

$$h(p) \equiv \hat{f}(p)/\hat{f}(0) \equiv 1 - H(p) = 1 - ca_0^2 p^2 + \dots \quad (3.23)$$

Here c is a positive constant of order 1. Recall that $f(x)$ damps rapidly out of the region $0 < x < a_0$.

Near the critical point, $b \sim b_c = 1$, the two-point correlation function behaves as

$$\begin{aligned} \hat{G}_{\kappa_0}^{(2)}(p) &= \frac{b}{\hat{f}(0)} \frac{1}{H(p) + \Delta bh(p)} \\ &\sim \frac{1}{H(p) + \langle N \rangle^{-1/2}}. \end{aligned} \quad (3.24)$$

Here we used Eq. (3.19). Thus the correlation length is $\xi = a_0 N^{1/4}$, which shows the first definition of the Hausdorff dimension defined in Eq. (2.15) to be $d_H^{(1)} = 4$. Let us consider the region

$$a_0 \ll x < \xi = a_0 N^{1/4}, \quad (3.25)$$

or, in momentum space,

$$\frac{1}{\xi} = N^{-1/4}/a_0 < p \ll 1/a_0. \quad (3.26)$$

a_0 gives an ultraviolet cutoff, whereas ξ gives an infrared cutoff length over which correlation functions damp rapidly. In the above scaling region of Eq. (3.26), the correlation function behaves as an ordinary massless field $\hat{G}_{\kappa_0}^{(2)}(p) \sim 1/p^2$, and gives the second definition of the Hausdorff dimension of Eq. (2.18), $d_H^{(2)} = 2$. This is different from the Hausdorff dimension $d_H^{(1)}$ determined from the relation of the system size N and the extent of the system. In Sec. III D, we show that the above behavior of the correlation function in the scaling region is not correct and hence gives the incorrect Hausdorff dimension $d_H^{(2)}$.

Finally, we consider $m > 2$ point correlation functions. As in the case of the two-point function, when m points are fixed on each tree graph, we can uniquely fix the path connecting these points. Therefore, an m -point function $\hat{G}_{\kappa_0}^{(m)}$ is represented as a summation over all tree diagrams with m fixed points in which $\hat{G}_{\kappa_0}^{(2)}(p)$ appear as propagators. For example,

$$\hat{G}_{\kappa_0}^{(3)}(p, q) = (\hat{G}_{\kappa_0}^{(1)})^{-2} \hat{G}_{\kappa_0}^{(2)}(p) \hat{G}_{\kappa_0}^{(2)}(q) \hat{G}_{\kappa_0}^{(2)}(p + q). \quad (3.27)$$

In general, we obtain the following result for m -point correlation functions;

$$\begin{aligned} \hat{G}_{\kappa_0}^{(m)} &\sim (\text{correlation functions of massless} \\ &\phi^3 \text{ theory at tree level}). \end{aligned} \quad (3.28)$$

D. Correlation functions in the thermodynamic limit

Let us consider the generalized m -point correlation functions with $l \geq 1$. From definition (3.8), they can be obtained by applying the l th derivative to the $l = 0$ case:

$$\begin{aligned} \hat{G}_{\kappa_0, l}^{(m)}(p^1, \dots, p^{m-1}) &= \left(\kappa_0 \frac{\partial}{\partial \kappa_0} \right)^l \hat{G}_{\kappa_0, l=0}^{(m)}(p^1, \dots, p^{m-1}) \\ &= \left(\frac{b}{1-b} \frac{\partial}{\partial b} \right)^l \hat{G}_{\kappa_0, l=0}^{(m)}(p^1, \dots, p^{m-1}). \end{aligned} \quad (3.29)$$

Partition functions are obtained from Eq. (3.21) as

$$Z_{\kappa_0, l} = \left(\frac{b}{1-b} \frac{\partial}{\partial b} \right)^{l-1} \frac{bV}{\hat{f}(0)}. \quad (3.30)$$

Near the critical point ($b_c = 1$), these become

$$Z_{\kappa_0, l \geq 2} \sim \frac{V}{\hat{f}(0)} \frac{(2l-5)!!}{(1-b)^{2l-3}}. \quad (3.31)$$

The two-point function with $l = 1$ is given by

$$\begin{aligned} \hat{G}_{\kappa_0, l=1}^{(2)}(p) &= \left(\frac{b}{1-b} \frac{\partial}{\partial b} \right) \left(\frac{b}{\hat{f}(0)[1-bh(p)]} \right) \\ &\sim \frac{1}{\hat{f}(0)} \frac{1}{(1-b)[1-bh(p)]^2} \\ &\sim \frac{1}{p^4}. \end{aligned} \quad (3.32)$$

This is due to the fact that in the scaling region [Eq. (3.26)] and near the critical point, the following inequality holds:

$$\frac{1}{b} \sim 1 \ll \frac{1}{1-bh(p)} \sim \frac{1}{c(a_0 p)^2 + N^{-1/2}} \ll \frac{1}{1-b} \sim \sqrt{N}. \quad (3.33)$$

This behavior is different from that of $\hat{G}_{\kappa_0, l=0}^{(2)} \sim 1/p^2$. Similarly, for $l \geq 2$, the behavior of the two-point function becomes

$$\begin{aligned} \hat{G}_{\kappa_0, l \geq 2}^{(2)}(p) &\sim \frac{1}{\hat{f}(0)} \frac{(2l-3)!!}{(1-b)^{2l-1}[1-bh(p)]^2} \\ &\times \left[1 + 2 \frac{1-b}{1-bh(p)} + 6 \frac{l-2}{2l-3} \left(\frac{1-b}{1-bh(p)} \right)^2 \right. \\ &\left. + \dots \right]. \end{aligned} \quad (3.34)$$

Due to inequality (3.33), the derivative $\partial/\partial b$ acts dominantly on $1/(1-b)$, not on $1/[1-bh(p)]$. The normalized two-point functions now become

$$\begin{aligned}
\hat{g}_{\kappa_0, l \geq 2}^{(2)}(p) &\sim \frac{1}{V} \frac{2l-3}{(1-b)^2} \frac{1}{[1-h(p)]^2} \\
&\times \left[\left(1 - 3 \frac{(1-b)^2}{2l-3} \frac{1}{[1-h(p)]^2} + \dots \right) \right. \\
&\sim \frac{\langle N \rangle}{V} \frac{1}{H(p)^2} \left(1 - 3 \frac{1}{\langle N \rangle} \frac{1}{H(p)^2} \right. \\
&\left. \left. + \mathcal{O} \left(\left(\frac{1}{\langle N \rangle H(p)^2} \right)^2 \right) \right) \right]. \quad (3.35)
\end{aligned}$$

Here we have used $\langle N \rangle = Z_{\kappa_0, l+1} / Z_{\kappa_0, l} = (2l-3)/(1-b)^2$ for the generalized grand canonical ensembles of l . Their p dependences are all the same except in the $l=0$ case. The $l=0$ case, which can be obtained directly from the Schwinger-Dyson equation, does not reproduce the correct thermodynamic result. Instead, we should consider a good grand canonical correlation function with $l \geq 1$; otherwise a nonuniversal small N behavior affects the summation and we cannot obtain the universal result. In Appendix B, we estimate the large N asymptotic behavior of the two-point function by the saddle point method. Such an explicit analytical result is completely consistent with the analysis here.

The behavior of $\hat{g}_{\kappa_0, l \geq 1}^{(2)}(p) \sim 1/p^4$ gives (the second definition of) the Hausdorff dimension [Eq. (2.18)] $d_H^{(2)} = 4$, which is now consistent with (the first definition of) the Hausdorff dimension discussed in Sec. III C. An argument expected from Fig. 3 is that the effect of branching could be absorbed by renormalizing the mass. If so, the propagator would behave like that of a random walk with a renormalized mass, and we might obtain a result identical to that of the $l=0$ case. In Sec. IV we discuss why this argument is not correct.

Similarly, three-point functions become

$$\begin{aligned}
\hat{g}_{\kappa_0, l=0}^{(3)}(p, q) &\sim g(p)g(q)g(p+q), \\
\hat{g}_{\kappa_0, l \geq 1}^{(3)}(p, q) &\sim g(p)'g(q)g(p+q) + g(p)g(q)'g(p+q) \\
&+ g(p)g(q)g(p+q)', \quad (3.36)
\end{aligned}$$

where

$$\begin{aligned}
g(p) &= \frac{1}{1-bh(p)} \sim \frac{1}{p^2}, \\
g'(p) &= \frac{1}{(1-bh(p))^2} \sim \frac{1}{p^4}. \quad (3.37)
\end{aligned}$$

The behaviors do not change above $l=1$. Only one propagator in a graph is replaced by $g'(p)$. This is because the derivative $\partial/\partial b$ dominantly acts on the factor $1/(1-b)$ rather than on $1/(1-bh(p))$, as in the case of two-point functions. For m -point functions ($m > 3$), we can obtain the same result.

$\hat{g}_{\kappa_0, l=0}^{(m)} \sim$ (correlation functions for ϕ^3 theory at tree level),

$\hat{g}_{\kappa_0, l \geq 1}^{(m)} \sim$ (correlation functions for ϕ^3 theory at tree level with a mass insertion). (3.38)

The universal correlation functions with $l \geq 1$ represent the correct correlation functions in the thermodynamic limit.¹

As a consistency check, the following relation between an $(m+1)$ -point function and an m -point function must hold:

$$\begin{aligned}
\hat{g}_{\kappa_0, l \geq 1}^{(m+1)}(p^1, \dots, p^{m-1}, p^m=0) \\
= \langle N \rangle \hat{g}_{\kappa_0, l \geq 1}^{(m)}(p^1, \dots, p^{m-1}). \quad (3.39)
\end{aligned}$$

It actually holds because on the left-hand side of Eq. (3.39), the special class of diagrams dominate in which the m th end point is attached to a propagator $g'(p)$. This is due to the inequality $g'(p=0)g(p) \gg g'(p)g(p=0)$. Therefore, it is equal to the right-hand side of Eq. (3.39).

IV. PHYSICAL INTERPRETATION BY A SINGLE MOTHER UNIVERSE

In this section, we give a physical interpretation of why the propagator behaves as $1/p^4$ instead of $1/p^2$. As we can see from Fig. 3, the effect of branching seems to be absorbed by renormalizing the mass, and we might conclude that the two-point function behaves like that of a random walk. If this is the case, the propagator should be given by an ordinary massive scalar particle with a renormalized mass $(a_0 N^{1/4})^{-1}$, instead of $(a_0 N^{1/2})^{-1}$. Similarly, higher point correlation functions should be given by tree graphs of ϕ^3 field theory. As we saw in Sec. III, these are not the correct behaviors for correlations. In this section, we give a physical interpretation of why the propagator behaves as $1/p^4$ instead of a conventional behavior $1/p^2$ and why the higher point correlation functions behave as in ϕ^3 theory with a single mass insertion.

Let us consider the two-point function as an example. The two-point function $\hat{G}_{\kappa_0}^{(2)}(p)$ was defined by a sum of two-point functions in the canonical ensemble [Eq. (3.14)]:

$$\hat{G}_{\kappa_0}^{(2)}(p) = \sum_{N=1}^{\infty} \kappa_0^N \hat{G}_N^{(2)}(p). \quad (4.1)$$

On the other hand, from Eq. (3.22), the function is written as a sum of all contributions over s , where s is the length between the two points in concern. Each term $\hat{G}_{\kappa_0}^{(1)}$ is represented by a gray blob in Fig. 3. When we fix the total number of the system N , the N points are distributed among $s+1$ blobs. We will show here that the most dominant contribu-

¹If we took the generalized ensemble [Eq. (3.8)] as a real physical system, we could see a phase transition at $l=l_c$ ($0 < l_c \leq 1$). Above l_c , the system size grows as κ approaches to κ_c , while it does not grow below l_c .

tions to the correlation functions are those in which most of N points are concentrated on only a single blob. We call this blob the mother universe. In the branched polymer, there is only one mother universe, and the other universes (blobs) contain much fewer points than the mother universe.

To show this, we first note that the one-point function (blob) is expanded as

$$\hat{G}_{\kappa_0}^{(1)} = \sum_{n=1}^{\infty} \kappa_0^n u_n, \quad (4.2)$$

where u_n is given at large n as

$$u_n = G_n^{(1)} \sim \frac{n^{-3/2} \hat{f}(0)^{n-1} e^n}{\sqrt{2\pi}}. \quad (4.3)$$

By using this expansion and Eq. (3.22), we obtain the two-point function for fixed N as

$$\hat{G}_N^{(2)}(p) = \sum_{s=0}^{\infty} \hat{f}(p)^s \left(\sum_{n_0=1}^{\infty} \cdots \sum_{n_s=1}^{\infty} u_{n_0} \cdots u_{n_s} \delta_{N, n_0 + \cdots + n_s} \right). \quad (4.4)$$

Each contribution in the brackets comes from a graph in which the first blob contains n_0 points, the second n_1 points, and so on. Using Eq. (4.3), the term in the brackets becomes

$$\begin{aligned} & \left(\frac{1}{\sqrt{2\pi}} \right)^{s+1} \hat{f}(0)^{N-s-1} e^N \\ & \times \sum_{n_0=1}^{\infty} \cdots \sum_{n_s=1}^{\infty} n_0^{-3/2} n_1^{-3/2} \cdots n_s^{-3/2} \delta_{N, n_0 + \cdots + n_s}. \end{aligned} \quad (4.5)$$

In the case of $s=1$, the summation

$$\sum_{n=1}^{N-1} n^{-3/2} (N-n)^{-3/2}. \quad (4.6)$$

is dominated in terms of $n \sim 0$ and $n \sim N$. For the general case with the exponent α ,

$$\sum_{n=1}^{N-1} n^\alpha (N-n)^\alpha, \quad (4.7)$$

the sum is dominated at the boundaries for $\alpha < -1$ and asymmetry arises between two blobs. Conversely, for $\alpha > -1$, N points are distributed equally, and neither blob is special. This argument can be generalized to $s > 1$. To conclude, most N points belong to a single blob along the propagator. We then have to divide the propagator with length s at the mother universe. Since the other blobs contain only a finite number of points, the effect of branching, other than dividing the propagator into two pieces, is simply to renormalize the mass of the propagator. Hence the propagator behaves as a product of two ordinary ones with a renormalized mass:

$$\hat{G}_N^{(2)}(p) \sim \left(\frac{1}{p^2 + m^2} \right)^2. \quad (4.8)$$

We can also apply a similar argument for higher-point functions. If the effect of branching is only to renormalize the mass term, the higher-point correlation functions will be represented by diagrams of ϕ^3 theory with propagators $1/(p^2 + m^2)$, which is not the correct thermodynamic behavior of the correlation functions, as we saw in Sec. III. Similar to the case of two-point functions above, we can argue that there is only one mother universe in which most of the N points reside. Since only a single blob contains infinitely many points, we have to divide one of the propagators at the mother universe, and this propagator behaves as $1/(p^2 + m^2)^2$. This mother universe corresponds to the mass insertion. The other blobs contain a finite number of points, and the effect of branching can be absorbed into mass renormalization. This is the physical reason why the higher point correlation functions are represented by tree diagrams of ϕ^3 field theory with a single mass insertion.

The above statement that there is only one mother universe in the branched polymer is explained differently as follows. Let us again consider original branched polymer systems with N points and $N-1$ bonds. By counting the number of ways in which we can divide a branched polymer into two parts by cutting a bond, we obtain a relation

$$(N-1)Z_N/V = \hat{f}(0) \sum_{N'=1}^{N-1} [N'Z_{N'}/V][(N-N')Z_{(N-N')}/V]. \quad (4.9)$$

The factor $(N-1)$ on the left-hand side is interpreted as the number of bonds we can cut to divide the whole into two parts. The factors N' and $(N-N')$ on the right-hand side are interpreted as the number of points to which the bond connecting the two parts is attached. Since Z_N behaves as in Eq. (3.11) at large N ,

$$NZ_N/V \gg \hat{f}(0) \sum_{N'=N\epsilon}^{N(1-\epsilon)} [N'Z_{N'}/V][(N-N')Z_{(N-N')}/V], \quad (4.10)$$

which means the summation on the right-hand side of Eq. (4.9) is dominated by terms of $N' \sim 0$ or $N' \sim N$. This formula can be interpreted as follows. If we divide any graph into two parts by cutting some bond, we find only finite points in one of them, most of them belonging to the other part. The mother universe belongs to the larger part. Consider the two-point function as an example. By dividing the graph of Fig. 3 into two parts at some bond, we find that most points are dominantly distributed in only one of them.

We can apply the same procedure to the dominant part with infinite points. After repeating this several times to divide the total graph into several pieces, we find that only a single part consists of infinitely many points, and that the others consist of finite points. We can find out which blob in Fig. 3 is the mother universe when, after several repetitions, the dominant part with infinite points is detached from the path in Fig. 3. We can also apply the same argument to the higher-point functions. Here we point out the difference of the argument given here from that given for random surfaces [8]. Although a similar inequality appears for random surfaces, the factor N is absent on the left-hand side of inequality (4.10) in that case.

V. CONCLUSION AND DISCUSSION

In this paper we have shown that correlation functions for branched polymers are given by functions for ϕ^3 theory at tree level *with a single mass insertion*, if we take the thermodynamic limit correctly. It is not given by functions for ϕ^3 theory at the tree levels themselves. We have interpreted the single mass insertion as the presence of a single mother universe in branched polymers.

We have reviewed random walks in order to clarify the relation between the canonical and grand canonical ensembles. We have introduced generalized grand canonical ensembles which assign different weights for different system sizes. We have emphasized that a “good” grand canonical ensemble is one in which the ensemble average is dominated by systems of large size. In branched polymers, this criterion is not satisfied in the conventional grand canonical ensemble. Nevertheless we can consider good grand canonical ensembles in branched polymers. Our conclusion follows the universal prediction of good grand canonical ensembles. It represents the correct scaling behavior of the correlation functions in canonical ensembles of large system size N .

ACKNOWLEDGMENTS

This work was supported in part by a Grant-in-Aid for Scientific Research from the Ministry of Education, Science, and Culture of Japan, and by the National Science Foundation under Grant No. PHYS94-07194.

APPENDIX A

In this appendix, we derive the canonical ensemble partition function (3.2) from the Schwinger-Dyson equation (3.16). Let us solve b as a form of expansion in κ . Each coefficient is calculated to be

$$\begin{aligned} & \frac{1}{2\pi i} \oint_{\kappa=0} d\kappa \frac{b}{\kappa^{N+1}} \\ &= \frac{1}{2\pi i} \oint_{b=0} db (1-b) e^{-b} \frac{b}{(be^{-b})^{N+1}} \quad (A1) \\ &= \frac{N^{N-1}}{N!}. \quad (A2) \end{aligned}$$

Hence

$$\begin{aligned} \left(\frac{1}{\hat{f}(0)}\right)^{N-1} \hat{G}_N^{(2)}(p) &= \frac{1}{2\pi i} \int_{-\infty}^{\infty} dt \frac{t}{1/b - 1 + H(p)} e^{N[1 - (t^2/2)]} \\ &= \frac{e^N}{2\pi} \int_{-\infty}^{\infty} dt \frac{t^2(1 - 13t^2/36 + \dots)}{[H(p) - 2t^2/3 + \dots]^2 + t^2[1 - 13t^2/36 + \dots]^2} e^{-Nt^2/2} \\ &= \frac{N^{-3/2} e^N}{2\pi} \int_{-\infty}^{\infty} dt \frac{t^2(1 - 13t^2/36N + \dots)}{[H(p) - 2t^2/3N + \dots]^2 + t^2/N[1 - 13t^2/36N + \dots]^2} e^{-t^2/2}, \quad (B5) \end{aligned}$$

where $H(p) = 1 - h(p) \sim c(a_0 p)^2$. Hence the normalized correlation function becomes

$$b = \sum_{N=1}^{\infty} \frac{N^{N-1}}{N!} \kappa^N. \quad (A3)$$

From Eqs. (3.6), (3.14), and (3.17), b is expanded as

$$b = \hat{f}(0) \sum_{N=1}^{\infty} \frac{N}{V} Z_N \kappa^N. \quad (A4)$$

Comparing these two expansions, we obtain the result of Eq. (3.2).

APPENDIX B

In this appendix, we derive the two-point correlation function in the canonical ensemble for fixed but large N . Similar to the calculation in Appendix A, we can obtain the two-point function for a fixed N from Eq. (3.22);

$$\begin{aligned} \left(\frac{1}{\hat{f}(0)}\right)^N G_N^{(2)}(p) &= \frac{1}{2\pi i} \oint_{\kappa=0} d\kappa \frac{\hat{G}_{\kappa_0}^{(2)}(p)}{\kappa^{N+1}} \\ &= \frac{1}{2\pi i} \oint_{b=0} db \frac{1}{\hat{f}(0)} \frac{1-b}{1-bh(p)} b^{-N} e^{bN}. \quad (B1) \end{aligned}$$

This integration can be estimated for large N by the saddle point approximation. Since $b^{-N} e^{bN} = e^{N(b - \log b)}$, the saddle point is at $b = 1$. The steepest descent direction is along the imaginary direction. We change the variable from b to t around the saddle point as

$$b - \log b = 1 - \frac{t^2}{2}. \quad (B2)$$

The new parameter t is written in terms of b by

$$t = i(1-b) \left(1 + \frac{1-b}{3} + \frac{7}{36}(1-b)^2 + \dots \right). \quad (B3)$$

Solving this, we obtain

$$\frac{1}{b} - 1 = -it \left(1 - \frac{2}{3}it - \frac{13}{36}t^2 + \dots \right). \quad (B4)$$

Therefore, in the saddle point approximation, the correlation function becomes

$$\begin{aligned}\hat{g}_N^{(2)}(p) &= \frac{\hat{G}_N^{(2)}(p)}{Z_N} \\ &= \frac{N}{V} \int_{-\infty}^{\infty} \frac{dt}{\sqrt{2\pi}} \frac{t^2(1-13t^2/36N+\dots)}{[H(p)-2t^2/3N+\dots]^2+t^2/N[1-13t^2/36N+\dots]^2} e^{-t^2/2}\end{aligned}\quad (\text{B6})$$

$$= \frac{N}{V} \int_{-\infty}^{\infty} \frac{dt}{\sqrt{2\pi}} \frac{t^2}{H(p)^2-4t^2H(p)/3N+t^2/N} e^{-t^2/2} \left(1 + O\left(\frac{1}{N}\right)\right).\quad (\text{B7})$$

The correlation function for branched polymers behaves very differently from the case of simpler random walks. In the region $H(p) \ll 1$, it becomes

$$\hat{g}_N^{(2)}(p) \sim \frac{N}{V} \int_{-\infty}^{\infty} \frac{dt}{\sqrt{2\pi}} \frac{t^2}{H(p)^2+t^2/N} e^{-t^2/2}.\quad (\text{B8})$$

In the coordinate representation, the two-point correlation function behaves as

$$\begin{aligned}g_N^{(2)}(\mathbf{x}) &\sim \int d^d \mathbf{p} \frac{N}{V} \int_{-\infty}^{\infty} \frac{dt}{\sqrt{2\pi}} \frac{t^2}{p^4+t^2/N} e^{-t^2/2} \exp(i\mathbf{p} \cdot \mathbf{x}) \\ &= \int_{-\infty}^{\infty} \frac{dt}{\sqrt{2\pi}} t^2 e^{-t^2/2} \frac{1}{|x|^{d-4}} \int d^d \mathbf{p} \frac{\exp(i\mathbf{p} \cdot \mathbf{e}_x)}{p^4+t^2|x|^4/N} \\ &\sim \frac{1}{|x|^{d-4}} \int_{-\infty}^{\infty} \frac{dt}{\sqrt{2\pi}} t^2 \exp\left(-\frac{t^2}{2} - \frac{\sqrt{t}|x|}{\sqrt{2}N^{1/4}}\right).\end{aligned}\quad (\text{B9})$$

In the scaling region $1 \ll |x| \ll N^{1/4}$, the t integration is estimated to be some x -independent number:

$$g_N^{(2)}(\mathbf{x}) \sim \frac{1}{|x|^{d-4}}.\quad (\text{B10})$$

This result for the canonical ensemble is completely consistent with the result of the grand canonical ensemble [Eq. (3.35)].

On the other hand, for $|x| \gg N^{1/4}$, the second term in the exponential in the t integration dominates the first term, and gives another power behavior instead of exponential damping:

$$g_N^{(2)}(\mathbf{x}) \sim \frac{1}{|x|^{d+2}}.\quad (\text{B11})$$

This is due to the contribution of the massless component ($|t| \sim 0$). This has no analog in the random walk, where the correlation damps exponentially with mass of order $N^{1/2}$.

- [1] J. Fröhlich, in *Critical Phenomena, Random Systems, Gauge theories*, edited by K. Osterwaldr and R. Stora (Elsevier Science, Amsterdam, 1984), p. 727.
 [2] S. Nishigaki and T. Yoneya, Nucl. Phys. B **348**, 787 (1991).
 [3] P. Di Vecchia, M. Kato, and N. Ohta, Nucl. Phys. B **357**, 495 (1991).
 [4] A. Anderson, R.C. Myers, and V. Periwal, Nucl. Phys. B **360**, 463 (1991).
 [5] H. Aoki, S. Iso, H. Kawai, Y. Kitazawa, and T. Tada, Prog.

- Theor. Phys. **99**, 713 (1998); e-print hep-th/9802085.
 [6] N. Ishibashi, H. Kawai, Y. Kitazawa, and A. Tsuchiya, Nucl. Phys. B **498**, 467 (1997); e-print hep-th/9612115.
 [7] H. Aoki, S. Iso, H. Kawai, Y. Kitazawa, A. Tsuchiya, and T. Tada, Prog. Theor. Phys. Suppl. **134**, 47 (1999); e-print hep-th/9908038.
 [8] H. Kawai, Nucl. Phys. B, Proc. Suppl. **26**, 93 (1992).
 [9] H. Aoki, S. Iso, H. Kawai, and Y. Kitazawa, Prog. Theor. Phys. (to be published); e-print hep-th/9909060.